Wendelstein 7-X Program—Demonstration of a Stellarator Option for Fusion Energy

R. C. Wolf, C. D. Beidler, A. Dinklage, P. Helander, H. P. Laqua, F. Schauer, T. Sunn Pedersen, F. Warmer, and Wendelstein 7-X Team*

***Abstract*— The superconducting stellarator Wendelstein 7-X is currently being commissioned. First plasmas are expected for the second half of 2015. W7-X is designed to overcome the main drawbacks of the stellarator concept and simultaneously demonstrate its intrinsic advantages relative to the tokamak—i.e., steady-state operation without the requirement of current drive or stability control. An elaborate optimization procedure was used to avoid excessive neoclassical transport losses at high plasma temperature, while simultaneously achieving satisfactory equilibrium and stability properties at high β in combination with a viable divertor concept. In addition, fast-ion confinement must be consistent with the requirements of alpha-heating in a power plant. Plasma operation of Wendelstein 7-X follows a staged approach following the successive completion of the in-vessel components. The main objective of Wendelstein 7-X is the demonstration of steady-state plasma at fusion relevant plasma parameters. Wendelstein 7-X will address major questions for the extrapolation of the concept to a power plant. These include divertor operation at high densities, plasma fueling at high central temperatures, avoiding impurity accumulation, and an assessment of the effect of neoclassical optimization on turbulent transport and fast-ion confinement. A power plant concept based on an extrapolation from Wendelstein 7-X, the helical advanced stellarator, has been developed.**

***Index Terms*— Fusion power plant, steady-state magnetic confinement, stellarator.**

I. Introduction

MAGNETIC confinement in stellarators can be provided without a toroidal plasma current. A rotational transform is generated by magnetic field coils only. This has several advantages [1].

1) Steady-state confinement is provided without any current drive. Compared with a tokamak, this should significantly reduce the recirculating power in a stellarator power plant.
2) Current-driven instabilities and disruptions do not occur. Even if a significant bootstrap current is generated, the negative magnetic shear prevents the destabilization of neoclassical tearing modes [2]. As a result, elaborate stability control is not required.
3) Without strong toroidal plasma currents, the Greenwald density limit is not observed and at a given fusion power, the alpha-particle pressure and the drive for fast-ion driven instabilities are reduced. As a consequence, densities far beyond an equivalent Greenwald limit have been observed [3], [4].

However, stellarator confinement also has several disadvantages. In general, the coil configuration is more complicated. Generating the rotational transform by external coils breaks the toroidal symmetry. As a result, sufficient confinement of the thermal plasma and fast ions for a fusion reactor is not reached automatically. The neoclassical transport in the $1/\nu$-regime at low collisionality [5]

$$\chi_{1/\nu} \propto \varepsilon_{\text{eff}}^{3/2} T^{7/2} \Big/ \left(n R_0^2 B_0^2\right) \tag{1}$$

shows a very strong dependence on the plasma temperature T (R_0 is the major radius of the device, B_0 is the magnetic field on axis, and n is the plasma density). To avoid an unacceptable increase of the plasma transport at reactor relevant temperatures, a minimization of the effective ripple ε_{eff} in the design of a stellarator is mandatory. From (1), it also becomes clear that confinement benefits from high density and low temperature. Other optimization criteria for stellarators are the fast-ion confinement, plasma stability at high normalized pressure β, a plasma equilibrium that does not deteriorate with increasing β, and—as a prerequisite for steady-state operation—a feasible exhaust concept. With regard to fast-ion confinement, the ability to operate at high density is a positive feature of the stellarator, as it keeps the fast-ion population low.

From the technological point of view, it is important to find a coil configuration that is capable of producing a magnetic field simultaneously fulfilling these criteria. A technical solution to generate such magnetic field configurations are modular coils [6]. Finally, a reactor or power plant requires sufficient space for a breeding blanket between coils and plasma. This is a major constraint for a fusion power plant design.

II. Wendelstein 7-X Design

Wendelstein 7-X (W7-X) is a drift-optimized stellarator with improved neoclassical confinement [7]. An effective ripple, ε_{eff}, of about 1% at all plasma radii ensures that the neoclassical plasma transport, even at higher temperatures, remains

Manuscript received July 31, 2015; revised March 29, 2016; accepted April 28, 2016. Date of publication May 30, 2016; date of current version September 9, 2016. This work has been carried out within the framework of the EUROfusion Consortium and was supported by the Euratom Research and Training Programme 2014–2018 under Grant 633053. The views and opinions expressed herein do not necessarily reflect those of the European Commission.

R. C. Wolf, C. D. Beidler, A. Dinklage, P. Helander, H. P. Laqua, F. Schauer, T. Sunn Pedersen, and F. Warmer are with the Max-Planck-Institut für Plasmaphysik, Greifswald 17491, Germany (e-mail: robert.wolf@ipp.mpg.de; craig.beidler@ipp.mpg.de; andreas.dinklage@ipp.mpg.de; per.helander@ipp.mpg.de; heinrich.laqua@ipp.mpg.de; felix.schauer@ipp.mpg.de; thomas.sunn.pedersen@ipp.mpg.de; felix.warmer@ipp.mpg.de).

Color versions of one or more of the figures in this paper are available online at http://ieeexplore.ieee.org.

Digital Object Identifier 10.1109/TPS.2016.2564919

*For Wendelstein 7-X Team see author list of H.S. Bosch et al., Nucl. Fusion 53 (2013) 126001.

sufficiently low. Improved fast-ion confinement is provided by a quasi-isodynamic configuration, requiring high β to achieve improved confinement.

The basic philosophy of the W7-X equilibrium is to decouple the plasma equilibrium and plasma β as far as possible. This is achieved by minimizing bootstrap and Pfirsch–Schlüter currents. As a result, the Shafranov shift and the changes of the rotational transform profile $\iota(r)$ remain small when β is increased. The latter is closely linked to the exhaust concept. Establishing low magnetic shear with $\iota = 1$ at the plasma edge, large magnetic islands intersected by target plates serve as a divertor (so-called magnetic island divertor). The first magnetic island divertor was successfully tested in Wendelstein 7-AS [8]. One important characteristic is the very large target-to-target connection length of the open magnetic field lines in the scrape-off layer. Compared, for instance, with the poloidal divertor in ASDEX Upgrade, which has a connection length of about 50 m, the connection lengths in W7-X amount to about 300 m [9]. This should have a profound effect on the heat flux distribution on the divertor target plates [10].

W7-X has been designed for steady-state plasma operation. For this purpose, superconducting coils are employed. The actively cooled plasmafacing components are designed for heat fluxes ranging from 100 kW/m^2 (water cooled stainless steel panels) to 1 MW/m^2 (water cooled CuCrZr heat sinks covered with graphite tiles) and 10 MW/m^2 divertor targets [water cooled CuCrZr heat sinks covered with carbon fiber composite (CFC)]. A newly developed electron cyclotron resonance heating (ECRH) system provides up to a 9 MW steady-state heating power at 140 GHz corresponding to second-harmonic heating at 2.5 T. Limited by the overall cooling capability of the water cooling plant, 10 MW plasmas will be restricted to about 30 min pulse duration. Compared with present day devices, this is a significant step forward in steady-state plasma operation. All plasma time scales lie far below 30 min, confinement time and fast-ion slowing down time are below 1 s, and the L/R time is about 100 s at most.

The magnetic field configuration of W7-X is generated by 70 superconducting coils [11] (Fig. 1). Five essentially identical magnetic field modules form the toroidal coil arrangement. Fifty nonplanar coils (ten in each module) generate both toroidal and poloidal components of the magnetic field. Twenty planar coils (four in each module) are arranged in such a way that they produce vertical and toroidal magnetic field components. The vertical magnetic field can be used to change the radial position of the plasma, while the toroidal component modifies the rotational transform. Inside the plasma vessel, ten normally conducting saddle coils have been installed to provide divertor strike-point sweeping. Outside the cryostat vessel, providing cryogenic vacuum for the superconducting coils, five normally conducting trim coils can be used to correct low-order error fields or otherwise modify the control magnetic field components [12].

W7-X has a major radius of $R_0 = 5.5$ m and an effective minor radius of $\langle a \rangle = 0.55$ m. The resulting plasma volume is 30 m^3. The maximum magnetic field strength on axis is 3 T, corresponding to a magnetic field energy of approximately 600 MJ. The nominal field, which is the reference for second-harmonic ECRH, is 2.5 T. The total mass of the device amounts to 725 tons. Including the magnetic field coils and the support structure, the cold mass is 423 tons. The superconductor is made of NbTi operating at 4 K to produce the field values mentioned above.

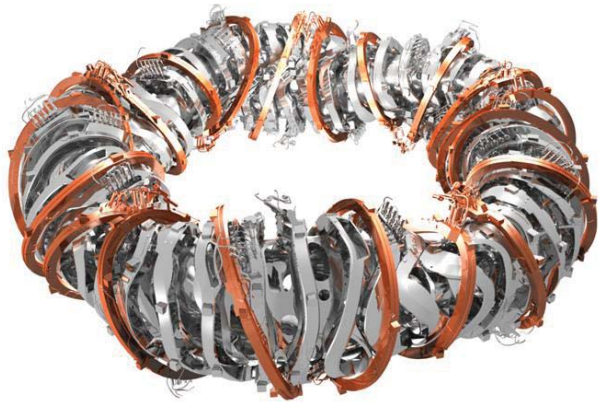

Fig. 1. Technical drawing of the W7-X magnetic field coils surrounding the plasma vessel. Fifty nonplanar coils (gray) and 20 planar coils (copper-colored) produce the confining magnetic field and can be used to change the rotational transform and the radial position of the plasma.

III. Approach to Steady-State Operation

The experimental capabilities of W7-X and the corresponding scientific program of W7-X are defined by the progress of the completion of the in-vessel components. Table I summarizes these capabilities and gives approximate values for the predicted plasma parameters. Accordingly, the program of W7-X until 2020, when the full steady-state capability is reached, is subdivided into distinct operational campaigns (OPs).

A. First Plasma (OP 1.1)

At present, W7-X is being commissioned [13]. The first plasma is expected in the second half of 2015.[1] During the operational phase, OP 1.1 up to 5 MW of ECRH power (at 140 GHz corresponding to 2.5 T) from six gyrotron tubes will be available. The plasma boundary will be defined by five in-board limiters, one in each module [Fig. 2(a)]. Integrated heating power and pulse duration are limited by the passive cooling capacity of these limiters.

The primary goal of OP 1.1 is the integral plasma commissioning of W7-X including ECRH and diagnostics. The draft physics plan foresees flux surface measurements, ECRH wall conditioning, and start-up optimization with helium, ECRH heated helium plasmas, first experience with hydrogen plasmas, and finally piggy-back experiments aiming at an even heat flux distribution among the five limiters, feedforward density control, and scrape-off layer physics. More detailed plans for OP 1.1 physics operation can be found in [14].

For OP 1.1, already six 140 GHz gyrotrons have been taken into operation delivering about 5 MW of heating power. The power transmission from the gyrotrons to the plasma relies

[1]First plasma was achieved on December 10, 2015, and OP 1.1 has been successfully completed by March 10, 2016.

TABLE I

SCIENTIFIC PROGRAM OF W7-X AND CORRESPONDING TECHNICAL CAPABILITIES AND PLASMA CHARACTERISTICS TOWARD STEADY-STATE OPERATION. TEMPERATURES, DENSITIES, AND β-VALUES ARE ESTIMATES PROVIDED BY TRANSPORT CALCULATIONS, ASSUMING NEOCLASSICAL TRANSPORT IN THE CORE OF THE PLASMA AND TURBULENT TRANSPORT AT THE PLASMA EDGE. IN THIS SENSE, THE β-VALUES ARE UPPER LIMITS

Year **Name of operational period** **(Duration)**	**Plasma configuration** **Plasma species** **Plasma characteristics**	**Available heating power and heating systems** **Predicted plasma temperatures, densities and β-values**
2015 OP 1.1 (13 weeks)	Limiter configuration He and H plasmas Pulse limit $\int P\,dt \leq 2$ MJ $\tau_{pulse} \sim 1$ s at 1 MW	$P \leq 5$ MW (ECRH) T_e (T_i) < 3 (1) keV $n < 0.2 \times 10^{20}$ m^{-3} $\beta < 1.6$ %
2017 / 18 OP 1.2 (60 weeks)	Uncooled divertor configuration (test divertor unit, TDU) H plasmas Pulse limit $\int P\,dt \leq 80$ MJ $\tau_{pulse} \sim 10$ s at 8 MW, (up to 60 s at reduced power)	$P \leq 10$ MW (ECRH, NBI, ICRH) T_e, T_i < 3 keV $n < 1.2 \times 10^{20}$ m^{-3} $\beta < 3$ %
> 2019 OP 2 ...	Steady-state operation Actively cooled HHF divertor H and D plasmas Divertor cryo-pump Heat flux limit P/A ≤ 10 MW/m^2 Technical limit $\tau_{pulse} \leq$ 30 minutes at 10 MW	P_{cw} ~9 MW (ECRH) P_{pulse} ~10 MW (NBI, ICRH, pulse length ~ 10 s) T_e, T_i < 5 keV $n < 2.4 \times 10^{20}$ m^{-3} $\beta < 5$ %

on a quasi-optical system (through air) [15]. It is characterized by an easy accessibility for alignment and maintenance. The overall power loss is about 3%–5%. Four front-steering launchers (with altogether 12 launch positions) in the outboard midplane of W7-X deliver the power to the plasma. Poloidal steering angles of ±25° and toroidal steering angles from −15° to +35° or from +15° to −35° can be used for changing the (vertical) deposition position or for current drive (toroidal launch). The frequency of 140 GHz corresponds to a central deposition at 2.5 T. The temperature and β-values given in Table I are derived from 1-D transport calculations prescribing the density profile, calculating the ECRH power deposition profile, and assuming neoclassical transport in the core of the plasma and turbulent transport at the plasma edge [16], [17]. Since a possible turbulent transport contribution in the plasma core is neglected, these values can be regarded as upper limits.

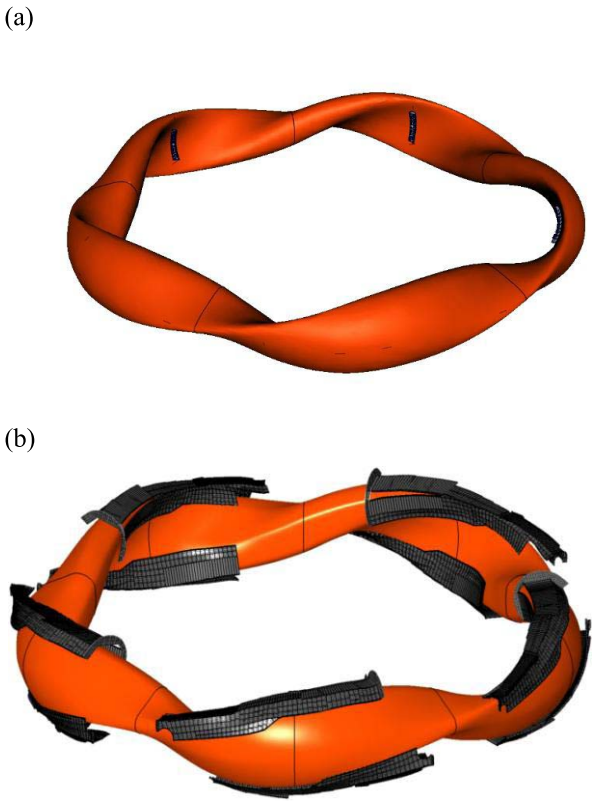

Fig. 2. (a) Plasma contour (orange) with five inboard limiters made of graphite (black stripes) defining the last closed flux surface. (b) Ten divertor units with the target plates following the topology of the resonant magnetic island divertor.

B. First Divertor Operation (OP 1.2)

Between OP 1.1 and OP 1.2, the limiters will be removed and a test divertor unit (TDU) made of graphite will be installed. In addition, the installation of the graphite tiles inside the plasma vessel will be completed. The TDU has already the shape of the actively cooled high heat flux divertor [see Fig. 2(b)], which will be installed by 2020. Since the TDU relies only on passive cooling, the pulse duration will be limited to about 10 s at 8 MW of heating power. However, the design without any water cooling is robust to heat flux overloading. Carbon sublimation and radiation collapse of the plasma would occur if excessive heat fluxes were to be present, but the divertor itself would remain functional. This serves the main goal of OP 1.2, which is the preparation of steady-state operation, gaining operational experience with the island divertor and developing and testing suitable monitoring and protection schemes. This goal already requires moderately high plasma densities. Using ECRH, the focus will be on second-harmonic X-mode (X2) heating, because this scheme has a single pass absorption of effectively 100%. Thus, the

X2 cutoff density of 1.2×10^{20} m^{-3} defines the upper limit of the density range of OP 1.2.

For OP 1.2, the ECRH system will be extended from six to ten gyrotrons, extending its capability from about 5 to 9 MW. In addition, two remote steering launchers (with two launch positions) will be installed [18]. Such launchers have very attractive properties for a fusion power plant. They have no movable parts near the plasma and exhibit a very high power density ($\sim$400 MW/m^2) requiring only little space to deliver high power levels. In W7-X, their launch direction is from the high field side. As a result, preferentially suprathermal electrons will be heated, allowing the energy dependence of electron confinement to be studied and also improving the current drive efficiency.

In addition to ECRH, neutral beam injection (NBI) [11] and ion cyclotron resonance heating (ICRH) [19] will become available. These heating systems will allow only pulsed operation with pulse durations of around 10 s. Applying NBI and ICRH, fast-ion populations can be generated, allowing first fast-ion confinement studies. Since the total heating power will be limited to about 10 MW (by the availability of power supplies), the achievable β-values will limit the exploitation of the quasi-isodynamic optimization and also the possibility of studying β-limiting stability phenomena.

C. Development of Integrated Steady-State Plasmas (OP2)

For OP2 and subsequent operational phases W7-X will have reached its full steady-state capability. The TDU will be replaced by the actively cooled high heat-flux (HHF) divertor. In addition, the water cooling of all plasma-facing components will be completed. Steady-state heating will be provided by ECRH. To reach plasma densities beyond the X2 cutoff ($n_e > 1.2 \times 10^{20}$ m^{-3}) second-harmonic O-mode heating has to be applied. For this purpose the W7-X ECRH system has been equipped with dedicated polarization optics to change from X2 to O2 heating when the cutoff density is reached. Since single pass absorption of O2 heating, depending also on plasma temperature, is on the order of 80%, W7-X is equipped with special in-vessel mirrors to facilitate efficient multi-pass absorption. Plasma densities beyond the O2 cutoff ($n_e > 2.4 \times 10^{20}$ m^{-3}) will require Bernstein wave heating.

The main objective of W7-X will be the development of an integrated steady-state scenario which demonstrates the reactor capability of the concept. This involves several aspects that combine the verification of the optimization criteria and issues not directly covered by the optimization such as density control and viable divertor performance.

1) Confinement and Stability: A central task is the verification of the neoclassical confinement optimization. According to theoretical predictions, β-values of 4% can be reached with 15 MW of heating power [16]. A very interesting question is how neoclassical optimization of ε_{eff} affects turbulent transport. 3-D calculations of ion-temperature-gradient-driven turbulence suggest a critical gradient similar to tokamaks, but with much reduced temperature profile stiffness [20], [21]. An interesting question, which the W7-X results will have to answer, is whether an H-mode transport barrier [22] at the plasma edge will be required to achieve sufficiently good confinement. Regarding MHD stability, W7-X plasmas are predicted to be stable against pressure-driven modes up to volume averaged β-values of $\langle\beta\rangle \approx 5\%$ [23]. To investigate this, however, the most recent numerical predictions show that the upgrades of the heating power including power supplies must have been completed.

2) Fast-Ion Confinement: With the availability of fast ion producing heating systems (NBI and ICRH), first fast ion studies can be started. However, to fully exploit the isodynamic effects on fast-ion confinement, β-values above 3% and the corresponding heating power to reach those β-values are required. Using NBI for fast-ion production has the intrinsic problem that with increasing density the NBI deposition moves to larger radii shifting the fast-ion orbits to regions where they are less confined [24]. Because high β requires improved neoclassical confinement, which in turn implies high density, NBI is not ideal to study fast-ion confinement. In contrast, the power deposition of ion-cyclotron minority heating is independent of the plasma density. However, at high plasma densities, the production of a sufficiently large fast-ion tail becomes more difficult. Here, dedicated studies are ongoing. A possibility of increasing the efficiency of the ion-cyclotron resonance frequency absorption might be a new three-ion-species plasma heating scheme that has been recently proposed [25]. While the problem to produce a fast-ion tail makes the demonstration of fast-ion confinement difficult in W7-X, this high-density feature of effective thermalization of fast-ion populations is of course a desired effect in a power plant.

3) Density and Impurity Control: As elaborated above, the full exploitation of the neoclassical confinement optimization [see (1)] requires high density. In addition, neoclassical transport predicts hollow density profiles if the temperature profiles are sufficiently peaked [26], [27]. Therefore, a suitable fueling scheme will have to be established. For this purpose, first pellet injection studies will be started in OP 1.2. To avoid hollow density profiles in plasmas of several kiloelectronvolts, central temperature steady-state high-speed pellet injection might become necessary. Finally, strong density gradients in combination with good neoclassical confinement show a tendency of impurity accumulation [28]. At high density, a negative electric field (ion-root confinement) is expected to cause impurity accumulation. This has in the past been avoided by suitable plasma scenarios such as the high density H-mode (HDH) discovered in Wendelstein 7-AS [29]. However, up to now, a clear theoretical understanding of the HDH-mode is missing, which makes it impossible to predict how it will scale to W7-X.

4) Establishing Equilibria for High-Power Divertor Operation: For its primary mode of operation, the W7-X magnetic island divertor requires $\iota = 1$ and low magnetic shear at the plasma boundary. The bootstrap current is not negligible for all magnetic field configurations, which can be realized in W7-X. A finite bootstrap current has the effect that the plasma equilibrium and thus the divertor configuration, and in particular the strike point positions evolve during the initial phase of a plasma pulse (on the L/R time scale,

which is on the order of 30 s). To avoid undue heat fluxes on the edges of the divertor tiles, which are not designed for 10 MW/m^2, mitigation schemes have been proposed. These include a so-called scraper element protecting these edges or electron cyclotron current drive [30], [31]. To test the mitigation schemes during OP 1.2, two of the ten divertor units will be equipped with such a scraper element. A possible upgrade for a later operational phase would be actively cooled scraper elements for the HHF divertor. Another issue, related to the divertor, is the balance between the power reaching the divertor target plates by heat conduction and convection and the radiated power fraction. In particular, going to power levels above 10 MW, safe divertor operation is expected to require a high radiated power fraction with at least partial detachment.

An integrated steady-state plasma scenario that simultaneously addresses all these issues will have to be developed. Concerning reactor-relevant plasma-facing materials, an upgrade to an all-metal wall will become necessary at a later stage (after OP2). For OP2, all plasma-facing components are made of stainless steel, amorphous carbon, or CFC. This selection was chosen because experience with an all-metal wall in stellarators is missing and impurity accumulation has been an issue in previous experiments. A stepwise coverage with tungsten, similar to the approach realized in ASDEX Upgrade [32], is envisaged when sufficient experience with plasma–wall interaction and impurity transport has been gained with the OP2 first wall configuration.

Concerning further upgrades of the steady-state heating power, ECRH launchers, parts of the transmission optics and the gyrotron building, already foresee two additional gyrotrons, increasing the number of microwave beams from 10 to 12. Combined with developing new gyrotrons, which, similar to the ITER gyrotrons, are designed for a power of 1.5 MW, this would increase the power level by almost a factor of two.

IV. Extrapolation to a Power Plant

A direct extrapolation from W7-X to a power plant is the helical advanced stellarator (HELIAS) [33], [34]. Recent studies focus on the HELIAS-5B [35]–[37], which like W7-X has fivefold symmetry (Fig. 3). The aspect ratio is similar to W7-X, the major radius is 22 m, and the average minor radius is 1.8 m. The average magnetic field lies in the range of 5 to 6 T with a maximum at the coils ranging from 10 to 12 T. From the engineering point of view, 6 T on axis seem feasible. However, to ease the requirements for the support structure and to save costs, lower values are desirable. The size of the coils and the magnetic field are similar to the ITER values, enabling the use of the ITER coil technology [38] including the superconductor material and the magnetic field values. Bolted panels between the coils form the coil support structure [39]. For the further improvement of the fast-ion confinement, stronger coil shaping might become necessary. Considering the space constraints, a possible solution could be a high-temperature superconductor with a higher current density. Staying at the moderate magnetic field strength of such a stellarator, a conductor with a higher current density would result in a reduced cross section of the coil. With regard to β, no extrapolation is necessary from W7-X to the HELIAS-5B. Both are designed for $\langle\beta\rangle \approx 5\%$. The fusion power is approximately 3 GW. For the blanket and shield, 1.3 m between the plasma and the coils has been reserved. First studies of a maintenance concept indicate sufficient accessibility between the coils and the coils support structure [36]. Neutronic analysis and studies of the blanket concept have been started (in collaboration with the Karlsruhe Institute of Technology).

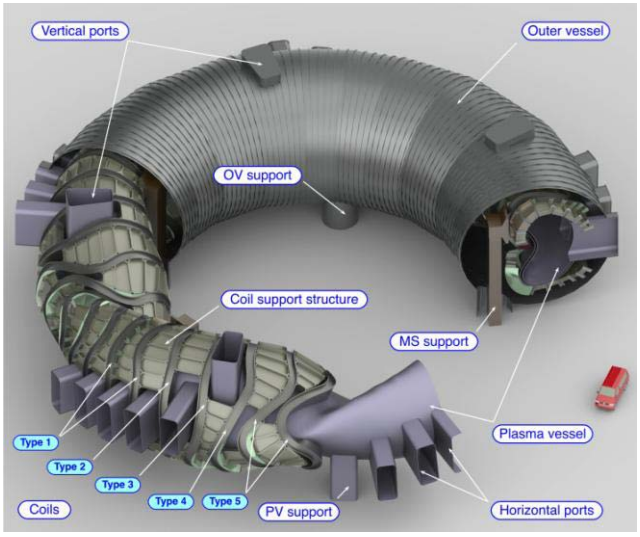

Fig. 3. Technical drawing of a HELIAS-5B power plant concept [36]. Shown are the plasma vessel, the five different coil types, the coil support structure, the magnet system support, and the outer cryostat vessel. The horizontal and vertical ports are indicated to demonstrate that the coils and the coil support structure permit large-scale access to the plasma vessel.

Considering that the HELIAS has the features of a power plant, an important question is how to bridge the gap from W7-X to such a power plant. Representing the Wendelstein line (W7-AS, W7-X, and HELIAS) in dimensionless engineering parameters [40] as was done before for ITER-like tokamaks [41], it becomes clear that the gap from W7-X to a HELIAS might need to be bridged by a stellarator burning-plasma experiment. The main objective of such an experiment would be to demonstrate significant α-heating without undue α-losses, requiring a birth profile that is consistent with regions of good α-confinement. The final step to a commercial power plant would then rely on the parallel development of the tokamak line and in particular on the transfer of the technologies of a tokamak demonstration power plant (DEMO) to a HELIAS [43].

The decision to go forward with such an experiment will await the results of W7-X high-power steady-state operation. Another factor influencing such a decision is the expected improvement of the capability to make theoretical predictions and extrapolations.

V. Conclusion

The scientific program of W7-X is determined by the completion of the plasma-facing components. Starting with a limiter configuration, plasma commissioning in 2015 has

aimed at the integral commissioning of the device including plasma heating with ECRH and the first set of plasma diagnostics. The second step is a divertor configuration without water cooling. In this phase, plasma pulses are limited to 10 s at 8 MW of heating power. The main goal is the preparation of the steady-state phase. Having reached the full steady-state capability in 2020, the main objective of W7-X is to demonstrate the power plant capability of the stellarator concept. This combines high-performance steady-state operation (high $nT\tau_E$) and the development of fully integrated plasma scenarios at high β for the extrapolation to a power plant. Upgrades introducing a tungsten wall and extending the steady-state heating power are envisaged.

In the European Roadmap to the Realization of Fusion Energy [42], the role of W7-X is to provide the input for the decision on a burning-plasma stellarator, which, in parallel to the tokamak DEMO, forms the basis for the development of a commercial fusion power plant.

REFERENCES

[1] P. Helander *et al.*, "Stellarator and tokamak plasmas: A comparison," *Plasma Phys. Control. Fusion*, vol. 54, no. 12, p. 124009, 2012.

[2] M. C. Zarnstorff *et al.*, "Physics of the compact advanced stellarator NCSX," *Plasma Phys. Control. Fusion*, vol. 43, no. 12A, p. A237, 2001.

[3] M. Hirsch *et al.*, "Major results from the stellarator Wendelstein 7-AS," *Plasma Phys. Control. Fusion*, vol. 50, no. 5, p. 053001, 2008.

[4] T. Morisaki *et al.*, "Superdense core mode in the large helical device with an internal diffusion barrier," *Phys. Plasmas*, vol. 14, no. 5, p. 056113, 2007.

[5] C. D. Beidler *et al.*, "Benchmarking of the mono-energetic transport coefficients–results from the international collaboration on neoclassical transport in stellarators (ICNTS)," *Nucl. Fusion*, vol. 51, no. 7, p. 076001, 2011.

[6] W. Wobig and S. Rehker, "A stellarator coil system without helical windings," in *Proc. 7th Symp. Fus. Technol.*, Grenoble, France, Oct. 1972, pp. 333–343.

[7] C. Beidler *et al.*, "Physics and engineering design for Wendelstein VII–X," *Fusion Sci. Technol.*, vol. 17, no. 1, pp. 148–168, 1990.

[8] P. Grigull *et al.*, "First island divertor experiments on the W7-AS stellarator," *Plasma Phys. Control. Fusion*, vol. 43, no. 12A, p. A175, 2001.

[9] Y. Feng, "Up-scaling the island divertor along the W7-stellarator line," *J. Nucl. Mater.*, vol. 438, pp. S497–S500, Jul. 2013.

[10] Y. Feng, M. Kobayashi, T. Lunt, and D. Reiter, "Comparison between stellarator and tokamak divertor transport," *Plasma Phys. Control. Fusion*, vol. 53, no. 2, p. 024009, 2011.

[11] H.-S. Bosch *et al.*, "Technical challenges in the construction of the steady-state stellarator Wendelstein 7-X," *Nucl. Fusion*, vol. 53, no. 12, p. 126001, 2013.

[12] T. Rummel *et al.*, "The trim coils for the Wendelstein 7-X magnet system," *IEEE Trans. Appl. Supercond.*, vol. 22, no. 3, Jun. 2012, Art. no. 4201704.

[13] F. Schauer *et al.*, "W7-X commissioning: Progress and lessons learned for future devices," in *Proc. 26th Symp. Fusion Eng.*, 2015, pp. 1–8, paper SX4-2.

[14] T. S. Pedersen *et al.*, "Plans for the first plasma operation of Wendelstein 7X," *Nucl. Fusion*, vol. 55 no. 12, p. 126001, 2015. [Online]. Available: http://dx.doi.org/10.1088/00295515/55/12/126001

[15] V. Erckmann *et al.*, "Electron cyclotron heating for W7-X: Physics and technology," *Fusion Sci. Technol.*, vol. 52, no. 2, pp. 291–312, 2007.

[16] Y. Turkin *et al.*, "Neoclassical transport simulations for stellarators," *Phys. Plasmas*, vol. 18, no. 2, p. 022505, 2011.

[17] J. Geiger, C. D. Beidler, Y. Feng, H. Maaßberg, N. B. Marushchenko, and Y. Turkin, "Physics in the magnetic configuration space of W7-X," *Plasma Phys. Control. Fusion*, vol. 57, no. 1, p. 014004, 2015.

[18] V. Erckmann, "ECRH and W7-X: An intriguing pair," in *Proc. AIP Conf.*, vol. 1580. 2014, p. 542, doi: 10.1063/1.4864608.

[19] J. Ongena *et al.*, "Study and design of the ion cyclotron resonance heating system for the stellarator Wendelstein 7-X," *Phys. Plasmas*, vol. 21, no. 6, p. 061514, 2014.

[20] P. Xanthopoulos *et al.*, "Controlling turbulence in present and future stellarators," *Phys. Rev. Lett.*, vol. 113, p. 155001, Oct. 2014.

[21] P. Helander *et al.*, "Advances in stellarator gyrokinetics," *Nucl. Fusion*, vol. 55, no. 5, p. 053030, 2015.

[22] F. Wagner, M. Hirsch, H.-J. Hartfuss, H. P. Laqua, and H. Maaßberg, "H-mode and transport barriers in helical systems," *Plasma Phys. Control. Fusion*, vol. 48, no. 5A, p. A217, 2006.

[23] C. Nührenberg, "Global ideal magnetohydrodynamic stability analysis for the configurational space of Wendelstein 7–X," *Phys. Plasma*, vol. 3, no. 6, p. 2401–2410, 1996.

[24] M. Drevlak, J. Geiger, P. Helander, and Y. Turkin, "Fast particle confinement with optimized coil currents in the W7-X stellarator," *Nucl. Fusion*, vol. 54, no. 7, p. 073002, 2014.

[25] Y. O. Kazakov, D. Van Eester, R. Dumont, and J. Ongena, "On resonant ICRF absorption in three-ion component plasmas: A new promising tool for fast ion generation," *Nucl. Fusion*, vol. 55, no. 3, p. 032001, 2015.

[26] H. Maaßberg, C. D. Beidler, and E. E. Simmet, "Density control problems in large stellarators with neoclassical transport," *Plasma Phys. Control. Fusion*, vol. 41, no. 9, p. 1135, 1999.

[27] A. Dinklage *et al.*, "Inter-machine validation study of neoclassical transport modelling in medium- to high-density stellarator-heliotron plasmas," *Nucl. Fusion*, vol. 53, no. 6, p. 063022, 2013.

[28] H. Maaßberg *et al.*, "Transport in stellarators," *Plasma Phys. Control. Fusion*, vol. 35, p. B319, 1993.

[29] K. McCormick *et al.*, "New advanced operational regime on the W7-AS stellarator," *Phys. Rev. Lett.*, vol. 89, p. 015001, Jun. 2002.

[30] A. Lumsdaine, "Design and analysis of the W7-X divertor scraper element," *Fusion Eng. Des.*, vol. 88, nos. 9–10, pp. 1773–1777, Oct. 2013.

[31] J. Geiger *et al.*, "Aspects of steady-state operation of the Wendelstein 7-X stellarator," *Plasma Phys. Control. Fusion*, vol. 55, no. 1, p. 014006, 2013.

[32] R. Neu *et al.*, "Overview on plasma operation with a full tungsten wall in ASDEX Upgrade," *J. Nucl. Mater.*, vol. 438, pp. S34–S41, Jul. 2013.

[33] C. D. Beidler *et al.*, "The Helias reactor HSR4/18," *Nucl. Fusion*, vol. 41, no. 12, p. 1759, 2001.

[34] R. C. Wolf and The Wendelstein 7X Team, "A stellarator reactor based on the optimization criteria of Wendelstein 7-X," *Fusion Eng. Des.*, vol. 83, pp. 990–996, Dec. 2008.

[35] F. Schauer, H. Wobig, K. Egorov, V. Bykov, and M. Köppen, "Extrapolation of the W7-X magnet system to reactor size," *Contrib. Plasma Phys.*, vol. 50, no. 8, pp. 750–755, 2010.

[36] F. Schauer, K. Egorov, and V. Bykov, "HELIAS 5-B magnet system structure and maintenance concept," *Fusion Eng. Des.*, vol. 88, pp. 1619–1622, Oct. 2013.

[37] F. Warmer *et al.*, "HELIAS module development for systems codes," *Fusion Eng. Des.*, vol. 91, pp. 60–66, Feb. 2015.

[38] F. Schauer, K. Egorov, and V. Bykov, "Coil winding pack FE-analysis for a HELIAS reactor," *Fusion Eng. Des.*, vol. 86, pp. 636–639, 2011.

[39] F. Schauer, K. Egorov, V. Bykov, and A. Dudek, "Building block support structure for HELIAS Stellarator reactors," in *Proc. IEEE/INPSS 24th Symp. Fusion Eng. (SOFE)*, Jun. 2011, pp. 1–6, paper SP 1-18.

[40] A. Dinklage *et al.*, "The initial programme of Wendelstein 7-X on the way to a HELIAS fusion power plant," in *Proc. 25th IAEA Fusion Energy Conf.*, 2014, paper FIP 3-1.

[41] K. Lackner, "Dimensionless engineering variables for measuring the ITER and reactor relevance of tokamak experiments," *Fusion Sci. Technol.*, vol. 54, no. 4, pp. 989–993, 2008.

[42] *Fusion Electricity, A Roadmap to the Realisation of Fusion Energy*, accessed on Nov. 2012. [Online]. Available: http://www.eurofusion.org/wpcms/wp-content/uploads/2013/01/JG12.356-web.pdf

[43] H. Zohm, "Assessment of DEMO challenges in technology and physics," *Fusion Eng. Des.*, vol. 88, nos. 6–8, pp. 428–433, Oct. 2013, doi: dx.doi.org/10.1016/j.fusengdes.2013.01.001.

Authors' photographs and biographies not available at the time of publication.